



Bioscientia Medicina: Journal of Biomedicine & Translational Research

Journal Homepage: www.bioscmed.com

Metabolic Dysfunction Precedes Dopaminergic Loss in Early MSA-C: A Discordant ¹⁸F-FDG PET and ^{99m}Tc-TRODAT-1 Case Study

Arvian Muhammad Barid^{1*}, Kharisma Perdani¹, Trias Nugrahadi¹, A Hussein S Kartamihardja¹

¹Department of Nuclear Medicine and Molecular Theranostics, Faculty of Medicine, Universitas Padjadjaran/Dr. Hasan Sadikin General Hospital, Bandung, Indonesia

ARTICLE INFO

Keywords:

¹⁸F-FDG PET

^{99m}Tc-TRODAT-1

Glial cytoplasmic inclusions

Multiple system atrophy

Neurodegeneration

*Corresponding author:

Arvian Muhammad Barid

E-mail address:

arvian.mb@gmail.com

All authors have reviewed and approved the final version of the manuscript.

<https://doi.org/10.37275/bsm.v10i4.1551>

ABSTRACT

Background: Differentiating early-stage multiple system atrophy-cerebellar type (MSA-C) from other ataxia syndromes presents a significant diagnostic challenge. While striatal dopaminergic denervation is a hallmark of synucleinopathies, it may be absent in the early stages of the cerebellar subtype. This study investigates the temporal dissociation between metabolic and dopaminergic biomarkers. **Case Presentation:** We report a 48-year-old male presenting with a 5-year history of progressive cerebellar ataxia and mild Parkinsonism, resistant to dopaminergic therapy. Written informed consent was obtained from the patient for the publication of this case details and images. To exclude mimics, a basic metabolic workup and High-resolution 3T MRI were performed. MRI revealed mild cerebellar atrophy but lacked the specific hot cross bun sign. Wilson's disease screening was negative. Due to limited resources, advanced genetic panels for spinocerebellar ataxias were not performed. The patient underwent dual-modality molecular imaging. On Day 1, ¹⁸F-FDG PET/CT demonstrated profound hypometabolism in the cerebellum (Cerebellum/Whole-Brain SUVr: 0.68) and pons (SUVr: 0.72). Conversely, on Day 30, ^{99m}Tc-TRODAT-1 SPECT revealed robust, symmetrical striatal uptake with Specific Binding Ratios (SBR) of 1.15 (Right) and 1.12 (Left), indicating preserved presynaptic dopamine transporter density. **Conclusion:** This case illustrates a critical temporal dissociation in MSA-C pathophysiology: widespread pontocerebellar metabolic failure occurs prior to structural nigrostriatal degeneration. Clinicians must recognize that a normal DAT scan does not exclude MSA-C. In limited-resource settings where genetic testing is unavailable, ¹⁸F-FDG PET offers superior sensitivity in the early diagnostic window to support the diagnosis.

1. Introduction

Multiple system atrophy (MSA) stands as one of the most enigmatic and devastating entities within the spectrum of neurodegenerative proteinopathies. Historically fragmented into distinct eponymous disorders—Shy-Drager syndrome, striatonigral degeneration, and olivopontocerebellar atrophy—it is now unified as a single, relentlessly progressive, sporadic, adult-onset disorder. The clinical phenotype is notoriously protean, characterized by a variable and debilitating combination of autonomic failure,

levodopa-resistant Parkinsonism, cerebellar ataxia, and pyramidal signs.¹ Unlike idiopathic Parkinson's disease (PD), which may offer a comparatively prolonged disease course managed by dopaminergic replacement, MSA is marked by a rapid functional decline, with a mean survival of only 6 to 9 years from symptom onset.²

The fundamental neuropathological substrate of MSA distinguishes it sharply from other synucleinopathies.³ While PD and Dementia with Lewy Bodies are characterized by the intraneuronal

accumulation of alpha-synuclein in the form of Lewy bodies, MSA is defined as a primary gliopathy. The hallmark lesion is the glial cytoplasmic inclusion (GCI), also known as the Papp-Lantos body. These inclusions represent the accumulation of misfolded, phosphorylated alpha-synuclein within oligodendrocytes—the myelinating support cells of the central nervous system.⁴ The implications of this cellular specificity are profound; oligodendrocytes are crucial for the metabolic support of axons, particularly in high-energy demand tracts. The pathological cascade in MSA, therefore, begins with oligodendroglial dysfunction, leading to myelin instability, subsequent axonal degeneration, and finally, secondary neuronal death. This neurodegenerative process does not affect the brain uniformly. Based on the predominant distribution of this pathology and the resulting motor phenotype, MSA is clinically categorized into two major subtypes: the parkinsonian variant (MSA-P), associated with predominant striatonigral degeneration, and the cerebellar variant (MSA-C), associated with olivopontocerebellar atrophy (OPCA). While MSA-P predominates in Western populations, MSA-C is more prevalent in Asian cohorts, presenting a unique set of diagnostic challenges. In MSA-C, the burden of GCIs is heavily concentrated in the pontine nuclei, inferior olivary nuclei, and cerebellar hemispheres, disrupting the intricate feedback loops necessary for motor coordination before significantly encroaching upon the nigrostriatal dopaminergic pathways.⁵

Diagnosing MSA-C in its nascent stages is a task fraught with complexity. The clinical presentation of early-onset ataxia combined with subtle extrapyramidal signs creates a broad differential diagnosis that overlaps significantly with idiopathic PD, late-onset cerebellar ataxias (LOCA), and hereditary spinocerebellar ataxias (SCAs). In the absence of a definitive post-mortem histopathological examination, clinicians must rely on consensus criteria—most recently updated by the Movement Disorder Society (MDS)—which stratify diagnosis into clinically established, clinically probable, and possible

categories.⁶ However, clinical evaluation alone often lacks the sensitivity to distinguish early MSA-C from its mimics. For instance, the autonomic dysfunction central to MSA may be subtle or subclinical in the early phases, manifesting only as erectile dysfunction or urinary urgency, which are non-specific in middle-aged populations. Furthermore, the structural imaging hallmark of MSA-C—the hot cross bun sign on T2-weighted magnetic resonance imaging (MRI), representing cruciform pontine gliosis—is highly specific but notoriously insensitive in early disease. Studies indicate that significant pontine atrophy often lags behind clinical symptoms, rendering standard MRI non-diagnostic during the critical window where therapeutic or supportive interventions are most needed. In resource-limited settings, where genetic panels to exclude the vast array of SCAs are unavailable or cost-prohibitive, the diagnostic uncertainty is further compounded, necessitating a reliance on functional biomarkers to phenotype the disease process.⁷

In this diagnostic vacuum, *in vivo* molecular imaging has emerged as an indispensable tool for early stratification, allowing clinicians to visualize pathophysiology before it manifests as gross structural atrophy. Two primary single-photon emission computed tomography (SPECT) and positron emission tomography (PET) modalities are utilized to interrogate the functional status of the motor control networks: ¹⁸F-Fluorodeoxyglucose PET (¹⁸F-FDG PET) and dopamine transporter (DAT) imaging. ¹⁸F-FDG PET serves as a marker of regional cerebral glucose metabolism, which acts as a proxy for synaptic activity and neuro-glial coupling. In MSA-C, metabolic mapping has proven to be a superior early biomarker. The metabolic signature of MSA-C is distinct and severe: hypometabolism in the cerebellum, brainstem (pons and medulla), and middle cerebellar peduncles.⁸ Crucially, this metabolic failure is thought to reflect the burden of alpha-synuclein within the oligodendrocytes and the resulting synaptic dysfunction, occurring well before the neurons degenerate to the point of visible atrophy on MRI.

Conversely, DAT imaging (utilizing tracers such as ^{123}I -FP-CIT or $^{99\text{m}}\text{Tc}$ -TRODAT-1) is designed to evaluate the integrity of presynaptic nigrostriatal dopaminergic terminals. In idiopathic PD and MSA-P, the loss of these terminals is a cardinal feature, resulting in reduced striatal uptake even in the premotor phases of the disease. Consequently, a reduced DAT signal is widely accepted as a confirmation of degenerative Parkinsonism, while a normal scan is frequently interpreted as evidence against a neurodegenerative etiology, often steering the diagnosis towards psychogenic movement disorders, drug-induced Parkinsonism, or essential tremor.

It is within the specific context of MSA-C that the standard diagnostic algorithms relying on DAT imaging begin to falter. While nigrostriatal degeneration is an eventual feature of almost all MSA cases, the temporal sequence of this degeneration varies significantly between subtypes. In MSA-P, the substantia nigra is an early casualty. However, in MSA-C, the degenerative epicenter is the olivopontocerebellar system. Emerging literature and longitudinal cohorts have identified a diagnostic blind spot: a subset of patients with clinically probable MSA-C who present with normal presynaptic dopaminergic imaging.⁹ Recent estimates suggest that 20% to 40% of patients with early clinical MSA-C may preserve nigrostriatal integrity during the initial years of the disease. This phenomenon implies the existence of a pre-nigral or pre-striatal phase of MSA-C, where the pathological burden is confined to the hindbrain and cerebellum, sparing the midbrain dopaminergic neurons until later stages. This discordance—positive metabolic signs of degeneration in the cerebellum (via FDG PET) alongside negative signs of degeneration in the striatum (via DAT SPECT)—poses a significant risk of misdiagnosis. A clinician relying solely on a normal DAT scan might erroneously exclude MSA, delaying appropriate management. This discrepancy highlights a critical pathophysiological insight: the synaptic and metabolic failure of the cerebellar network occurs temporally prior to the retrograde or trans-synaptic

degeneration of the nigrostriatal dopamine system. Understanding this timeline is vital not only for diagnostic accuracy but also for understanding the spreading mechanism of prion-like alpha-synuclein strains, which appear to propagate through specific connectomes at different rates.¹⁰

This study aims to elucidate the pathophysiological timeline of early-stage Multiple System Atrophy-Cerebellar type through a detailed examination of a temporally discordant case. We present the distinct clinical scenario of a 48-year-old male exhibiting progressive ataxia and Parkinsonism, in whom profound cerebellar and pontine hypometabolism on ^{18}F -FDG PET was observed despite completely preserved dopaminergic transporter density on $^{99\text{m}}\text{Tc}$ -TRODAT-1 SPECT. By integrating these findings within the context of a limited-resource setting—where advanced genetic exclusion of SCAs was not feasible—we highlight the superior sensitivity and indispensable value of metabolic imaging over transporter imaging in the early diagnostic window. This report serves to alert clinicians to the limitations of DAT SPECT in cerebellar presentations and underscores the utility of ^{18}F -FDG PET as a definitive biomarker for the pre-nigral phase of MSA-C.

2. Case Presentation

Written informed consent was obtained from the patient for the publication of this case report and any accompanying images. A 48-year-old male presented to the Nuclear Medicine department on January 2025 (Day 1), referred by a movement disorder neurologist for the evaluation of suspected atypical Parkinsonism versus hereditary ataxia. The patient reported a 5-year history of progressive motor dysfunction, initially manifesting as mild lower limb stiffness and gait instability, which had significantly exacerbated over the preceding three years. The primary complaints included involuntary movements of the legs while seated, persistent lower limb rigidity throughout the day, and subjective weakness during physical activity. The patient reported distinct unsteadiness when turning and frequent stumbling. Review of systems

was negative for tinnitus, hearing loss, headache, vertigo, paresthesia, or cognitive decline. Importantly, there was no history of orthostatic fainting, though urinary urgency was reported. There was no history of trauma, CNS infection, cerebrovascular accidents, or toxin exposure. The family history was negative for movement disorders, ataxia, or early-onset dementia, suggesting a sporadic etiology. The patient was currently managed with Pramipexole 0.25 mg once daily but reported minimal to no symptomatic relief. This lack of response to dopamine agonists serves as a clinical hallmark suggestive of atypical Parkinsonism rather than responsive idiopathic PD.

Upon presentation to the Nuclear Medicine department, the 48-year-old male patient appeared alert and fully oriented to time, place, and person, reflected in a maximum Glasgow Coma Scale (GCS) score of E4V5M6. Anthropometric evaluation revealed a body weight of 60 kg and a height of 175 cm, resulting in a Body Mass Index (BMI) of 19.6 kg/m². While falling within the lower range of normal, this BMI is clinically relevant in the context of neurodegenerative synucleinopathies, where unintended weight loss and a catabolic state can often precede or accompany motor progression. The neurological examination dissected the patient's intricate motor and non-motor deficits, revealing a multiple system involvement characteristic of atypical Parkinsonism. Cranial nerve examination was largely intact, with isochoric pupils and preserved light reflexes. However, oculomotor testing revealed a subtle but specific deficit: saccadic eye movements were notably hypometric. While nystagmus was absent, hypometric saccades implicated dysfunction within the dorsal vermis and the fastigial nucleus of the cerebellum, serving as an early clinical marker of cerebellar degeneration distinct from the oculomotor apraxia often seen in progressive supranuclear palsy (PSP). The motor examination identified a confluence of extrapyramidal and pyramidal signs. Increased tone, characterized as rigidity rather than spasticity, was evident in the lower extremities bilaterally. Concomitantly, deep tendon reflexes were

hyperreflexic (graded 3+) in both the knees and ankles. This hyperreflexia in the presence of rigidity is a pivotal clinical clue, pointing towards pyramidal tract involvement, which is a supportive feature of multiple system atrophy (MSA) that helps distinguish it from uncomplicated idiopathic Parkinson's disease (PD). Cerebellar testing confirmed significant dysfunction. While finger-to-nose testing demonstrated only mild dysmetria, heel-to-shin testing revealed profound ataxia, highlighting a disproportionate involvement of the lower limbs and vermis over the cerebellar hemispheres. The patient's gait was described as broad-based and unsteady, necessitating distinct caution during turning maneuvers.

To objectively quantify the disease burden, validated scales were employed: (1) UPDRS Part III (Motor Examination): The patient scored 18/108 in the OFF-medication state. A granular analysis of this score revealed that the total was driven primarily by axial instability and lower limb rigidity. Notably, the classic appendicular bradykinesia (slowness of finger tapping or hand movements) and resting tremor—hallmarks of PD—were largely absent. This phenotypic profile strongly suggested an atypical Parkinsonian syndrome; (2) SARA (Scale for the Assessment and Rating of Ataxia): The patient received a score of 8/40. This score objectively captures the distinct gait ataxia and stance instability, confirming that the cerebellar pathology was functionally symptomatic and not merely a radiological incidental finding; (3) Autonomic Interrogation: A critical component of the examination was the assessment of autonomic integrity. Orthostatic vital signs were measured after a supine-to-standing protocol. The systolic blood pressure demonstrated a precipitous drop of 25 mmHg (falling from 130/80 mmHg to 105/75 mmHg) upon standing for three minutes. This finding fulfills the consensus criteria for neurogenic orthostatic hypotension (defined as a drop of ≥ 20 mmHg systolic or ≥ 10 mmHg diastolic), confirming failure of the sympathetic baroreceptor reflex—a core clinical feature required for the diagnosis of MSA. Given the

patient's onset of symptoms at age 43 (five years prior to this presentation), he falls into the young-onset category for movement disorders. This necessitated a rigorous exclusion of hereditary, metabolic, and secondary causes that could mimic neurodegenerative ataxia.

A high-resolution 3.0 Tesla magnetic resonance imaging (MRI) scan of the brain was performed to assess for structural biomarkers. The imaging revealed a dichotomy between macrostructural atrophy and signal intensity changes: (1) T1-Weighted Sequences: These images demonstrated mild, generalized atrophy of the cerebellar vermis and hemispheres. This atrophy was deemed disproportionate to the patient's age of 48, supporting a degenerative etiology; (2) T2-Weighted and FLAIR Sequences: Crucially, the scan was scrutinized for the pathognomonic hot cross bun sign—a cruciform hyperintensity in the pons reflecting the degeneration of pontocerebellar fibers. This sign was absent. Furthermore, there was no hyperintensity along the putaminal rim, and the middle cerebellar peduncles (MCP) appeared isointense without the signal changes often seen in advanced MSA; The absence of the Hot Cross Bun sign does not exclude MSA, as this radiological marker has high specificity (approx. 97%) but low sensitivity (approx. 50-60%) in early-stage disease. The MRI findings were therefore interpreted as consistent with early cerebellar degeneration but non-diagnostic for confirmed MSA in isolation. The lack of other structural lesions (such as tumors, strokes, or demyelinating plaques) served to rule out secondary structural causes of ataxia.

The laboratory workup was targeted to exclude treatable mimics. In any movement disorder patient under age 50, Wilson's disease is a mandatory exclusion. The patient's serum ceruloplasmin was 28 mg/dL (well within the reference range of 20–60 mg/dL), and 24-hour urinary copper excretion was normal. A slit-lamp examination confirmed the

absence of Kayser-Fleischer rings, effectively ruling out hepatolenticular degeneration. It is important to note that due to the setting's resource limitations, comprehensive genetic panels for Spinocerebellar Ataxias (such as SCA 1, 2, 3, 6, 17) and paraneoplastic antibody screenings were not performed. Consequently, the diagnostic reliance shifted heavily toward the integration of the clinical phenotype (sporadic progression, autonomic failure) and the patterns observed on molecular imaging.

To definitively characterize the neurodegenerative process, the patient underwent a dual-modality functional imaging protocol (Figure 1). This approach revealed the study's central finding: a temporal dissociation between metabolic failure and dopaminergic structural loss. On Day 1, whole-body ¹⁸F-FDG PET/CT provided a map of regional cerebral glucose metabolism, a proxy for synaptic activity and neuronal health; (1) Qualitative Findings: Visual inspection showed preserved metabolism in the frontoparietal cortex and basal ganglia, arguing against cortical dementias (like Alzheimer's) or typical striatal degeneration. However, the scan revealed marked, symmetrical hypometabolism in the bilateral cerebellar hemispheres and the pons (Figure 2); (2) Quantitative Analysis (SUVr): Region of Interest (ROI) analysis validated the visual findings. Using the whole-brain mean as a normalization reference, the Cerebellum/Whole Brain Ratio was 0.68, significantly below the normal reference of >0.85. Similarly, the Pons/Whole Brain Ratio was 0.72 (Reference >0.82). In stark contrast, the Putamen/Whole Brain Ratio was 0.98, falling squarely within the normal range of 0.95–1.05; Interpretation: This pattern of selective pontocerebellar hypometabolism with striatal preservation is the specific metabolic signature of MSA-C. It suggests that the energy crisis and synaptic dysfunction in this patient are currently confined to the olivopontocerebellar network.

DIAGNOSTIC PATHWAY: EARLY MSA-C

Study Case: 48-Year-Old Male with Ataxia & Parkinsonism

Step 1: Clinical Presentation & Examination Day 1

- **Symptoms:** 5-year progressive ataxia, lower limb rigidity, poor levodopa response.
- **Signs:** Hypometric saccades, hyperreflexia (3+), broad-based gait.
- **Scores:** **SARA: 8/40** (Distinct Ataxia), **UPDRS III: 18/108** (Rigidity).
- **Autonomic:** Neurogenic Orthostatic Hypotension (-25 mmHg drop).

Step 2: Exclusionary Workup (Rule Out) Standard of Care

- **MRI Brain (3T):** Mild cerebellar atrophy. **Negative** for hot cross bun sign. No tumors/strokes.
- **Laboratory:** Ceruloplasmin 28 mg/dL (Normal). **Negative** for Wilson's Disease.
- **Note:** Genetic/Paraneoplastic panels unavailable (Resource Limited).

Step 3: ¹⁸F-FDG PET Metabolic Failure

- **Target:** Glucose Metabolism (Function)
- **Finding:** Marked Pontocerebellar Hypometabolism.
- **Data (SUVr):**
 - Cerebellum: **0.68** (Low)
 - Pons: **0.72** (Low)
- **Interpretation:** **Positive for MSA-C Pattern**

Step 4: ^{99m}Tc-TRODAT Structure Intact

- **Target:** Dopamine Transporter (Structure)
- **Finding:** Robust, Symmetrical Striatal Uptake.
- **Data (SBR):**
 - Right Striatum: **1.15** (Normal)
 - Left Striatum: **1.12** (Normal)
- **Interpretation:** **Negative for Nigral Degeneration**

⚠ THE DISCORDANCE ⚠

Metabolic Failure (PET) is present *before* Structural Dopaminergic Loss (SPECT).
Pre-Nigral Phase of MSA-C

Final Diagnosis: Probable MSA-C

Based on MDS Criteria (2022)

(Sporadic Ataxia + Autonomic Failure + Positive Metabolic Biomarker)

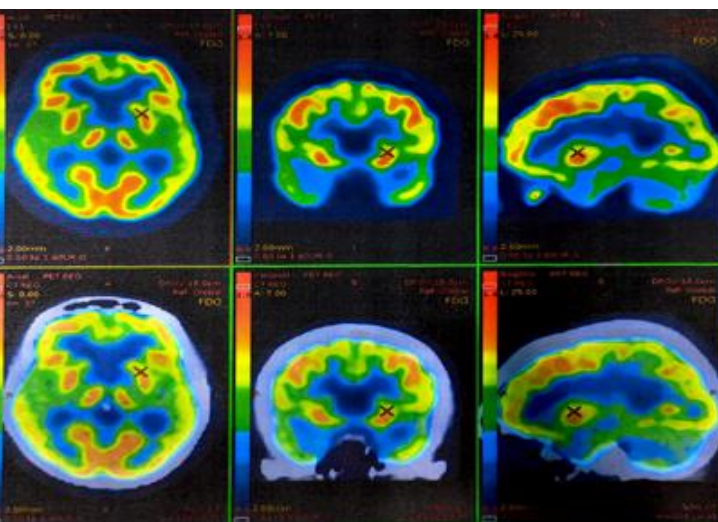


Figure 2. ¹⁸F-FDG PET/CT imaging revealed marked, symmetrical hypometabolism (cross symbol) in the bilateral cerebellar hemispheres and the pons.

Follow-up dopamine transporter (DAT) imaging was performed on Day 30 to assess the structural integrity of the nigrostriatal nerve terminals; (1) Qualitative Findings: The SPECT images displayed robust, high-contrast uptake in the striatum bilaterally. The uptake formed a symmetrical comma shape, indicating that both the head of the caudate and the putamen were intact (Figure 3). Notably, there was no amputation of the putaminal tail—the loss of posterior putaminal signal that is the earliest and most sensitive sign of typical Parkinson’s disease and

MSA-P; (2) Quantitative analysis (SBR): Specific binding ratios (SBR) were calculated using the occipital cortex as the background. The right striatum SBR was 1.15, and the left striatum SBR was 1.12, both well above the normal cutoff of >0.90; Interpretation: These values indicate intact presynaptic dopamine transporter density. The results are inconsistent with typical Parkinson’s Disease or advanced MSA-P, confirming that the patient’s Parkinsonian rigidity is likely not driven by nigrostriatal dopamine depletion at this stage.

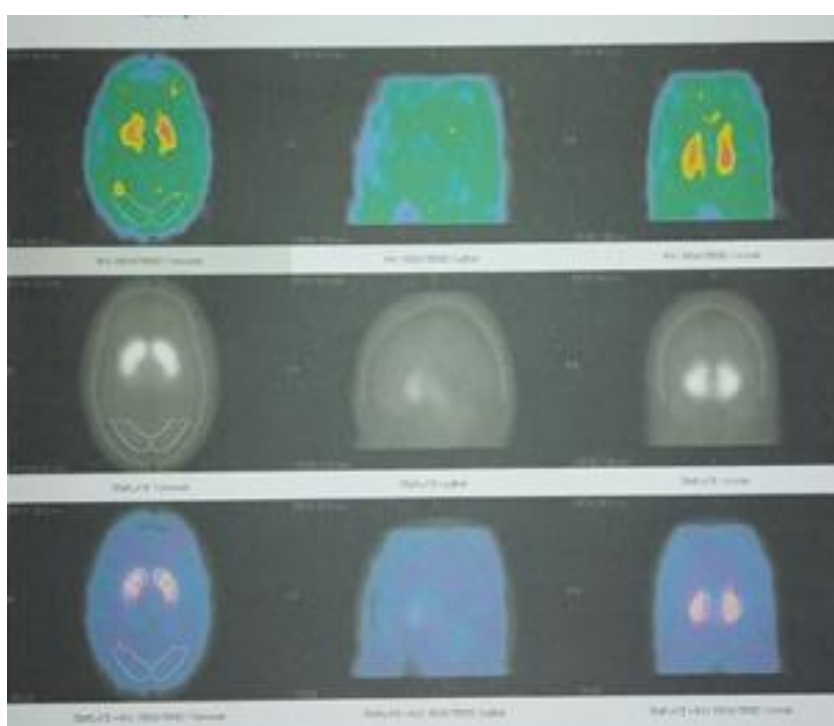


Figure 3. ^{99m}Tc TRODAT SPECT imaging displays a robust and symmetrical comma shape, indicating that both the head of the caudate and the putamen were intact.

The integration of these findings presents a cohesive diagnostic picture. The patient exhibits: (1) Sporadic, adult-onset progressive ataxia (SARA score 8/40); (2) Autonomic dysfunction, evidenced by neurogenic orthostatic hypotension; (3) Supportive biomarkers: A specific MSA-C pattern on FDG-PET (pontocerebellar hypometabolism). According to the Movement Disorder Society (MDS) criteria for multiple

system atrophy (2022), the combination of autonomic failure, cerebellar syndrome, and exclusion of alternative causes qualifies the patient for a diagnosis of probable MSA-C. The diagnosis is further refined by the molecular imaging discordance, suggesting the patient is in the pre-nigral phase of the disease, where metabolic failure in the cerebellum precedes the structural degeneration of the dopamine system.

3. Discussion

The clinical trajectory and diagnostic evaluation of the patient presented in this case study illustrate a profound and frequently overlooked diagnostic nuance in the field of movement disorders: the temporal and functional dissociation between metabolic network failure and structural nigrostriatal degeneration. This case challenges the prevailing binary diagnostic algorithms often employed in limited-resource settings, where a normal dopaminergic scan is frequently considered sufficient to exclude neurodegenerative Parkinsonism. By documenting a clear discordance between profound pontocerebellar hypometabolism on ^{18}F -FDG PET and completely preserved dopamine transporter density on $^{99\text{m}}\text{Tc}$ -TRODAT-1 SPECT, we provide compelling *in vivo* evidence for the pre-nigral phase of multiple system atrophy-cerebellar type (MSA-C). The following discussion dissects the pathophysiological mechanisms underlying this discordance, proposes a revised diagnostic hierarchy for resource-constrained environments, and explores the clinical implications of relying on single-modality imaging.¹¹

To understand why a patient would exhibit severe ataxia and metabolic brain failure while retaining a normal dopaminergic architecture, one must interrogate the unique cellular pathology of MSA. Unlike Parkinson's disease (PD), which is a primary neuronal synucleinopathy characterized by the accumulation of Lewy bodies within neurons, MSA is a primary gliopathy (Figure 4). The hallmark pathological feature is the Glial Cytoplasmic Inclusion (GCI), an aggregation of misfolded, fibrillar alpha-synuclein exclusively within oligodendrocytes.¹² This distinction is not merely histological; it is the driver of the disease's specific spatiotemporal progression. The GCI hypothesis posits that the pathological cascade in MSA is initiated by the dysfunction of oligodendrocytes. In the central nervous system, oligodendrocytes are not passive insulators; they are metabolically active partners to the axons they ensheath, providing critical trophic support and energy substrates (primarily lactate) to high-demand

neurons. In MSA-C, the burden of GCIs is disproportionately high in the white matter tracts of the cerebellum, pons, and inferior olives.¹³

As alpha-synuclein aggregates within these oligodendrocytes, their metabolic machinery begins to fail. This results in a starvation of the associated neuronal networks.¹⁴ The ^{18}F -FDG PET scan captures this event with high sensitivity. Glucose metabolism, as measured by FDG uptake, is a proxy for synaptic activity and the energy demand of the neuro-glial unit. In our patient, the profound hypometabolism observed in the cerebellum and pons (SUVr 0.68 and 0.72, respectively) reflects this primary oligodendroglial failure and the consequent synaptic quiescence. Importantly, this metabolic drop occurs functionally—it represents cells that are sick and metabolically downregulated, but not necessarily dead. Conversely, $^{99\text{m}}\text{Tc}$ -TRODAT-1 SPECT specifically images the dopamine transporter (DAT), a protein located on the presynaptic membrane of nigrostriatal nerve terminals. For the DAT signal to decrease, there must be a physical loss of these terminals or the nigral neurons themselves. In MSA-C, the degeneration of the substantia nigra is widely considered a secondary, downstream event, occurring either via retrograde dying-back axonopathy or trans-synaptic degeneration initiated by the failing striatal or cerebellar networks. Therefore, the discordance observed in this patient—Metabolic Failure (+) vs. Structural Integrity (-)—places him in a distinct pathophysiological window: the pre-nigral phase of MSA-C. At this stage, the olivopontocerebellar system has succumbed to the toxic effects of GCIs, leading to clinical ataxia and PET hypometabolism. However, the nigrostriatal dopaminergic neurons, while likely under stress, have not yet undergone sufficient apoptosis to reduce the density of dopamine transporters below the threshold of detection for SPECT imaging. This finding validates the hypothesis that in MSA-C, metabolic dysfunction is an upstream event that significantly predates the structural loss of the dopaminergic system.¹⁵

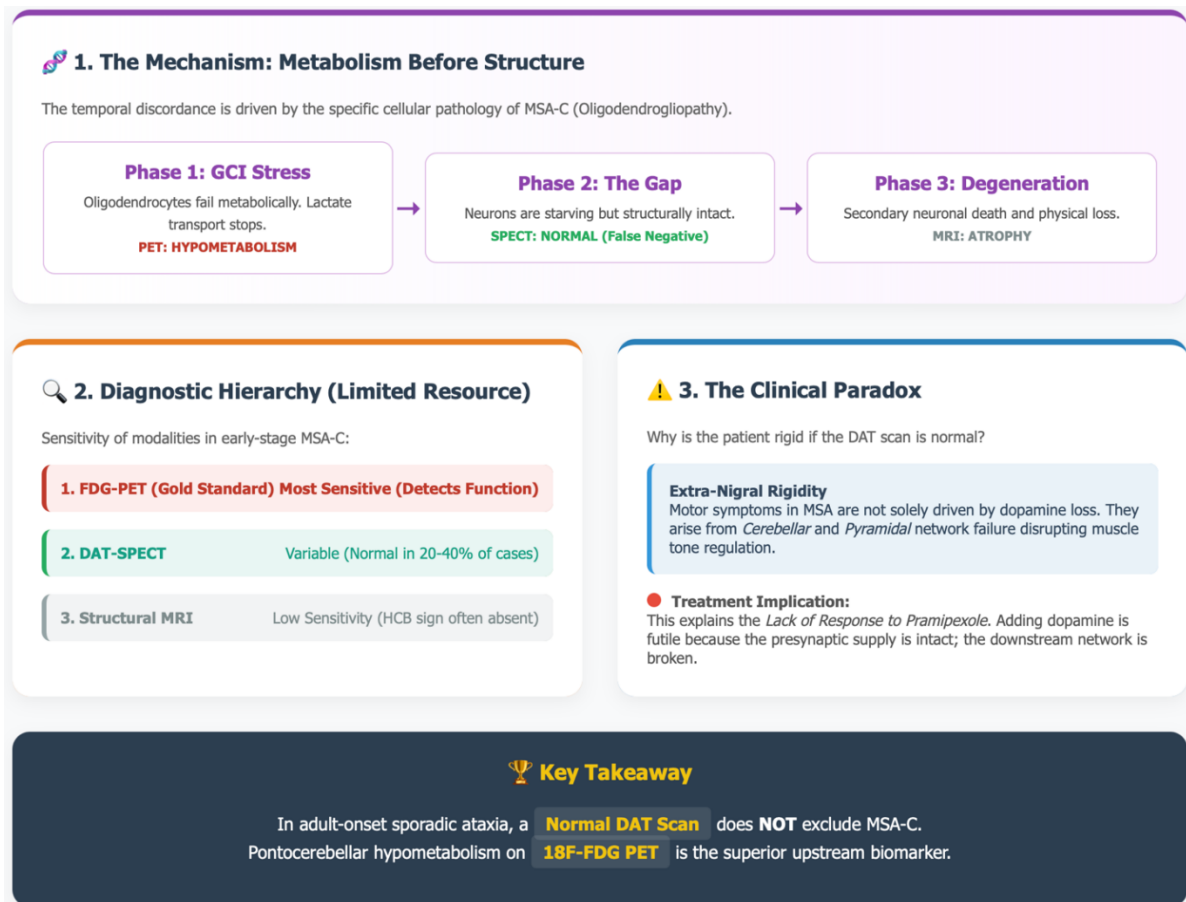


Figure 4. Discordant molecular imaging in early MSA-C.

In tertiary care centers equipped with genomic sequencing and research-grade biomarkers (such as alpha-synuclein seed amplification assays), the diagnosis of MSA is becoming increasingly refined. However, in limited-resource settings—which represent a significant portion of global medical practice—clinicians must rely on a hierarchy of accessible testing. This case highlights the strengths and critical failures of standard imaging modalities when applied to atypical Parkinsonism in such environments. Magnetic Resonance Imaging (MRI) is the standard first-line investigation for adult-onset ataxia.¹⁶ The search is typically for the hot cross bun sign (HCB), a cruciform T2-hyperintensity in the pons reflecting the degeneration of transverse pontine fibers. While the specificity of the HCB sign approaches 97–99%, its sensitivity is disappointingly

low in the early stages, estimated at only 50% to 60%. Our patient’s MRI showed mild atrophy but lacked this pathognomonic sign. A reliance on MRI can lead to false reassurance. In limited settings, a report of no hot cross bun sign observed is often misinterpreted as negative for MSA. This case reinforces that structural signs like the HCB are markers of advanced tissue destruction (gliosis and scarring). By the time the HCB sign is visible, the window for early intervention has closed. Thus, a negative MRI does not rule out MSA-C. Dopamine Transporter imaging (DaTscan or TRODAT-1) is frequently utilized as a binary filter: distinct reduction confirms neurodegeneration (PD, PSP, MSA), while normal uptake is presumed to indicate non-degenerative conditions (essential tremor, drug-induced parkinsonism, psychogenic). This binary heuristic fails in MSA-C. Studies by

Randel et al., Munoz et al., and others have demonstrated that up to 40% of patients with clinically probable MSA-C retain normal or borderline DAT binding at the onset of symptoms. The preservation of the nigrostriatal pathway in our patient (SBR > 1.1) despite clear rigidity and ataxia exemplifies this limitation. In a resource-limited setting, stopping the workup after a normal TRODAT scan would have led to a diagnostic error, potentially labeling the patient with a benign or psychogenic condition, thereby delaying appropriate counseling and management of autonomic risks. ¹⁸F-FDG PET emerged as the definitive arbiter in this case. By imaging metabolism rather than structure, PET detected the disease in its functional state.¹⁷

In the absence of genetic testing to rule out hereditary spinocerebellar ataxias (SCAs), the pattern of metabolism provides a highly specific fingerprint. Hereditary ataxias often show diffuse cortical or patchy hypometabolism, whereas MSA-C presents with a sharp, symmetrical pontocerebellar drop with relative preservation of the basal ganglia. This case supports a revised diagnostic hierarchy for limited-resource settings: In a patient with adult-onset ataxia and autonomic signs, if the MRI is non-diagnostic, the next step should ideally be FDG-PET, not DAT-SPECT.¹⁸ FDG-PET offers a one-stop assessment of the entire degeneration topography, whereas DAT-SPECT interrogates only a single neurotransmitter system that may be spared in the early disease course.

The clinical paradox presented by this patient—distinct Parkinsonian rigidity and levodopa resistance in the presence of a normal dopamine transporter scan—warrants careful clinical dissection. Traditionally, rigidity in Parkinsonism is attributed to the loss of nigrostriatal dopamine, which disinhibits the indirect pathway of the basal ganglia. However, if the DAT scan is normal, indicating preserved presynaptic dopamine terminals, why is the patient rigid? In MSA, motor symptoms are not solely driven by the nigrostriatal tract.¹⁹ The widespread degeneration of the cerebellum and the brainstem nuclei (including the pedunculo-pontine nucleus)

disrupts the extrapyramidal motor loops at multiple levels. Furthermore, the cerebellum exerts a tonic influence on muscle tone via the reticulospinal and vestibulospinal tracts. The profound cerebellar hypometabolism observed in this patient suggests that the braking mechanism of the cerebellum is failing, leading to increased tone and ataxia that mimics Parkinsonian rigidity. This distinction is vital: the rigidity is extra-nigral, arising from a network failure rather than a specific neurotransmitter deficiency. This pathophysiology explains the patient's poor response to Pramipexole (a dopamine agonist). Dopamine replacement therapies work by replenishing dopamine at the striatal receptors. In this patient, the presynaptic supply of dopamine is likely intact (as suggested by the normal TRODAT), and the primary dysfunction lies in the *processing* of motor signals by the cerebellum and downstream pathways. Therefore, adding more dopaminergic stimulation is physiologically futile. Clinicians should be cautioned that dopamine responsive dystonia or Parkinson's disease are not the only causes of rigidity. A lack of response to levodopa/agonists in a rigid patient with a normal DAT scan should not automatically trigger a diagnosis of psychogenic movement disorder. Instead, it should trigger an immediate referral for metabolic imaging to investigate atypical Parkinsonisms like MSA-C, where the pathology lies outside the dopaminergic synapse.²⁰

We acknowledge several limitations in this study that are inherent to its design and the clinical setting. First, this is a single case report. While it provides a deep phenotype of the pre-nigral window, the findings need validation in larger longitudinal cohorts to map the exact duration of this discordance. How long does the metabolic-structural gap last? Does it predict a slower or faster disease progression? Only longitudinal tracking can answer this. Second, definitive post-mortem histopathology—the gold standard for diagnosing GCI burden—is absent. However, the diagnosis of Probable MSA-C is robustly supported by the strict adherence to the MDS clinical criteria (sporadic onset, autonomic failure, cerebellar

syndrome). Third, and most notably, the study was conducted in a resource-limited environment where next-generation sequencing for hereditary Spinocerebellar Ataxias (SCAs) and comprehensive paraneoplastic antibody panels were unavailable. Theoretically, certain rare SCA subtypes (such as SCA 17 or SCA 2) can present with parkinsonism and ataxia. However, the specific combination of severe autonomic failure (neurogenic orthostatic hypotension) and the distinct pontine-sparing-striatal metabolic profile strongly favors MSA-C over hereditary mimics, which typically present with slower progression and different metabolic signatures. Rather than diminishing the value of the report, these limitations highlight the study's real-world relevance. Most clinicians do not practice in centers with unlimited access to genomic medicine. This case demonstrates how rigorous clinical phenotyping combined with judicious use of molecular imaging can achieve a high-probability diagnosis even when the perfect exclusion of mimics is not financially or logistically feasible.

4. Conclusion

The diagnostic journey of early-stage multiple system atrophy-cerebellar type is fraught with pitfalls, primarily due to the limitations of standard structural imaging and the variable sensitivity of dopaminergic functional imaging. This case report serves as a crucial didactic example of the discordant phenotype: a patient with clinical Parkinsonism and ataxia who exhibits a normal dopamine transporter scan (^{99m}Tc -TRODAT-1) but profound metabolic failure (^{18}F -FDG) in the cerebellum and pons. We conclude that the presence of intact presynaptic dopaminergic terminals does not exclude the diagnosis of MSA-C. Clinicians must recognize the pre-nigral phase of the disease, where pathology is confined to the olivopontocerebellar system. Cerebellar and pontine hypometabolism is an upstream, functional biomarker that detects the disease cascade—likely driven by oligodendroglial dysfunction—long before structural atrophy becomes visible on MRI or nigral degeneration

becomes visible on SPECT. In the diagnostic algorithm for adult-onset sporadic ataxia, particularly in limited-resource settings where genetic confirmation is not feasible, ^{18}F -FDG PET offers superior sensitivity and specificity compared to DAT-SPECT. Ultimately, this case advocates for a paradigm shift in the workup of atypical parkinsonism. When faced with a rigid, ataxic patient with a normal MRI and normal DAT scan, the clinician must not stop. The normal findings are not an end-point but a signal to look deeper into the metabolic landscape of the brain. Early identification via FDG-PET allows for accurate prognostication, appropriate management of autonomic comorbidities, and the potential inclusion of patients in future neuroprotective trials targeting the earliest phases of synucleinopathy.

5. References

1. Pitella FA, Alexandre-Santos L, de Lacerda KJCC, Trevisan AC, Kato M, Padovan-Neto FE, et al. Parkinson's disease and levodopa-induced dyskinesias: a quantitative analysis through ^{99m}Tc -TRODAT-1 SPECT imaging of the brain. *Radiol Bras.* 2024; 57: e20230082.
2. Wu D, Jiang Q, Shen G, Gao X, Liu C, Ye W. Quantitative analysis of striatal subregional asymmetry on ^{99m}Tc -TRODAT-1 SPECT and clinical correlations with UPDRS subscales in Parkinson's disease. *Ann Nucl Med.* 2025.
3. Huang W, Jiang H, Du Y, Wang H, Sun H, Hung G-U, et al. Transfer learning-based attenuation correction in ^{99m}Tc -TRODAT-1 SPECT for Parkinson's disease using realistic simulation and clinical data. *EJNMMI Phys.* 2025; 12(1): 43.
4. Su T-P, Huang C-J, Mao W-C, Chiu Y-H, Liu R-S, Chen L-F. Differentiating treatment-resistant depression with and without Parkinsonism in the elderly from a psychiatric perspective by ^{99m}Tc -TRODAT-1 SPECT imaging. *Int J Geriatr Psychiatry.* 2025; 40(6): e70102.

5. Mota W de O, Cardoso CD, Vasconcellos Neto JRT de, Silva MVCM. Efficacy and safety of ^{99m}Tc-Trodat-1 in the early and differential diagnosis of Parkinson's disease. *Delos*. 2025; 18(70): e6299.
6. Afonin GV, Glukhareva AE, Smolenov EI, Kolobaev IV, Beketov EE, Petrov LO, et al. The application of PET/CT with ¹⁸F-FDG in the differential diagnosis of lung solitary lesions. *Res N Pract Med J*. 2022; 9(3): 80–90.
7. Saponjski J, Macut D, Petrovic N, Ognjanovic S, Popovic B, Bukumiric Z, et al. Diagnostic and prognostic value of ^{99m}Tc-Tektrotyd scintigraphy and ¹⁸F-FDG PET/CT in a single-center cohort of neuroendocrine tumors. *Arch Med Sci*. 2023; 19(6): 1753–9.
8. Petrović J, Šobić-Šaranović D, Milovanović J, Jotić A, Odalović S, Grozdić-Milojević I, et al. The role of ¹⁸F-FDG PET/CT in the follow-up of laryngeal cancer after treatment. *Medicinska istraživanja*. 2023; 56(1): 1–8.
9. Kovacs DG, Ladefoged CN, Andersen KF, Brittain JM, Christensen CB, Dejanovic D, et al. Clinical evaluation of deep learning for tumor delineation on ¹⁸F-FDG PET/CT of head and neck cancer. *J Nucl Med*. 2024; 65(4): 623–9.
10. Muzi M, Peterson LM, Specht JM, Hippe DS, Novakova-Jiresova A, Lee JH, et al. Repeatability of ¹⁸F-FDG uptake in metastatic bone lesions of breast cancer patients and implications for accrual to clinical trials. *EJNMMI Res*. 2024; 14(1): 32.
11. Lavrova A, Pham NTT, Vernon CJ, Carlos AF, Petersen RC, Dickson DW, et al. A multimodal clinical diagnostic approach using MRI and ¹⁸F-FDG-PET for antemortem diagnosis of TDP-43 in cases with low-intermediate Alzheimer's disease neuropathologic changes and primary age-related tauopathy. *J Neurol [Internet]*. 2024; 271(7): 4105–18.
12. Lucic S, Spirovski M, Stojanovic D, Peter A, Licina J, Ivanov O, et al. ¹⁸F-FDG PET/CT- and MRI-based locally advanced cervical cancer early-response assessment after concurrent chemo- and radiotherapy-impact on patient outcomes and survival prediction. *Diagnostics (Basel)*. 2024; 14(13): 1432.
13. Lucic S, Spirovski M, Nikolin B, Stojanovic D, Peter A, Gajic B, et al. ¹⁸F-FDG PET/CT impact on malignant melanoma patients undergoing staging and restaging: a single-University-Center experience in a real-world setting. *Diagnostics (Basel)*. 2025; 15(12): 1560.
14. Krismer F, Seppi K, Jönsson L, Åström DO, Berger A-K, Simonsen J, et al. Sensitivity to change and patient-centricity of the unified multiple system atrophy rating scale items: a data-driven analysis. *Mov Disord*. 2022; 37(7): 1425–31.
15. Porto KJ, Hirano M, Mitsui J, Chikada A, Matsukawa T, Ishiura H, et al. COQ2 V393A confers high risk susceptibility for multiple system atrophy in East Asian population. *J Neurol Sci*. 2021; 429(117623): 117623.
16. Pellecchia MT, Stankovic I, Fanciulli A, Krismer F, Meissner WG, Palma J-A, et al. Can autonomic testing and imaging contribute to the early diagnosis of multiple system atrophy? A systematic review and recommendations by the Movement Disorder Society Multiple System Atrophy Study Group. *Mov Disord Clin Pract*. 2020; 7(7): 750–62.
17. Gu X, Chen Y, Zhou Q, Lu Y-C, Cao B, Zhang L, et al. Analysis of GWAS-linked variants in multiple system atrophy. *Neurobiol Aging*. 2018; 67: 201.e1-201.e4.
18. Kakumoto T, Orimo K, Matsukawa T, Mitsui J, Ishihara T, Onodera O, et al. Frequency of FGF14 intronic GAA repeat expansion in patients with multiple system atrophy and undiagnosed ataxia in the Japanese population. *Eur J Hum Genet*. 2025; 33(3): 325–33.

19. Zhao P, Zhang B, Gao S, Li X. Clinical features, MRI, and ¹⁸F-FDG-PET in differential diagnosis of Parkinson's disease from multiple system atrophy. *Brain Behav.* 2020; 10(11): e01827.
20. Hu X, Sun X, Hu F, Liu F, Ruan W, Wu T, et al. Multivariate radiomics models based on ¹⁸F-FDG hybrid PET/MRI for distinguishing between Parkinson's disease and multiple system atrophy. *Eur J Nucl Med Mol Imaging.* 2021; 48(11): 3469–81.